

# Coupling of Electromagnetic and Statistical Interactions for Two-Dimensional Electrons

Gabriel C. Magalhães<sup>1</sup>, Van Sérgio Alves<sup>1</sup>, E. C. Marino<sup>2</sup>, Leandro O. Nascimento<sup>3</sup>

<sup>1</sup> *Faculdade de Física, Universidade Federal do Pará,  
Av. Augusto Correa 01, Belém PA, 66075-110, Brazil*

<sup>2</sup> *Instituto de Física, Universidade Federal do Rio de Janeiro,  
C.P. 68528, Rio de Janeiro RJ, 21941-972, Brazil*

<sup>3</sup> *Faculdade de Ciências Naturais, Universidade Federal do Pará, C.P. 68800-000, Breves, PA, Brazil*

(Dated: December 21, 2024)

We study a nonlocal theory that describes both the electromagnetic and statistical interactions among two-dimensional electrons. This is shown through the effective action of the model. While the electromagnetic interaction is described by the so-called Pseudo Quantum Electrodynamics (PQED), the statistical part is obtained from the well-known Chern-Simons action. In the static limit, we show that the Chern-Simons parameter plays the role of an effective dielectric constant, which decreases the interaction in the large-screening limit. Thereafter, we apply the one-loop perturbation theory in our model. Within this approach, we calculate the electron self-energy, the electron renormalized mass, the corrected gauge-field propagator, and the renormalized Fermi velocity for both high- and low-speed limits, using the renormalization group.

PACS numbers: 12.20.Ds, 12.20.-m, 11.15.-q

## I. INTRODUCTION

Quantum electrodynamics (QED) is one of the most well-succeed theories in physics, in particular, because of the remarkable comparison between the experimental data for the electron  $g$ -factor and its theoretical prediction. Because the matter action is given by the Dirac theory, hence, most of its results are connected to electrons in particle physics. Recently, nevertheless, quantum electrodynamics has been shown a very useful tool in the physics of planar materials. Indeed, the experimental realization of graphene [1] has been an important bridge between quantum field theory and condensed matter physics in the last decade. The main reason is because of the low-energy excitations that behave as massless Dirac particles, with an effective velocity  $v_F \approx c/300$ , called Fermi velocity. This is a small fraction of the light velocity  $c$  [2]. The dynamics of electrons in graphene generates an experimental setup for observing the Klein tunneling at reasonable energy scales, in comparison with the energy scale in particle physics [3]. Beyond this large set of applications, new two-dimensional materials made that bridge even bigger than before. For instance, silicene, phosphorene, germanene, and the transition metal dichalcogenides [4] have been described by the massive Dirac theory at low energies. In literature, most of the applications have been discussed within a free-particle picture. On the other hand, a few applications have been made with some quantum-electrodynamical approach, in particular, the Pseudo Quantum Electrodynamics (PQED) has attracted great attention. The whole description of interactions, including those due to microscopic or statistical interaction, is still an open question in the physics of these planar materials.

It has been shown that PQED is the correct theory for describing electronic interactions among particles in

the plane. This is a nonlocal model generated by a dimensional reduction of QED, after constraining the electrons to the plane [5]. For the sake of consistency with quantum theory, it has been shown that PQED is unitary [6]. Furthermore, it yields the Coulomb potential  $V(r) \propto 1/r$  in the static limit, which is a desirable feature for applications in the physics of two-dimensional materials. Indeed, aiming for applications in condensed matter physics, several results have been obtained from this approach, for example, dynamical mass generation [7]; interaction driven quantum valley Hall effect [8]; quantum corrections of the electron  $g$ -factor [9]; Yukawa potential in the plane [10]; and electron-hole pairing (excitons) in transition metal dichalcogenides [11]. Nevertheless, all of these applications neglect the interaction of the matter with the Chern-Simons action at tree level. This interaction has been related to the effective action of the matter current, driven by the Chern-Simons action, after integrating out the gauge field. This effective action has been coined statistical interaction in Ref. [5]. The Chern-Simons model has an intrinsic parameter  $\theta$ , which yields a topological mass in the quantum electrodynamics in (2+1) dimensions (QED<sub>3</sub>), without breaking gauge symmetry [12].

In general grounds, the Chern-Simons action may be written either as an abelian or nonabelian gauge field. Here, we shall keep our attention only to the abelian case. The induction of the Chern-Simons action in the plane has been derived through a dimensional reduction of the topological action, derived from the Maxwell field. This action is given by the contraction of the electromagnetic field and its dual field. From this approach, it follows that the full interactions in the plane should include the  $\theta$ -parameter [5]. Another peculiar feature of the Chern-Simons theory is its induction, in the two-rank representation of the Dirac matrices, from one-loop quan-

tum corrections to the photon propagator in QED<sub>3</sub>. In this case, the induction of the Chern-Simons action is a realization of the so-called parity anomaly [8].

The interaction of the matter current with the Chern-Simons action yields a field theory for the Hall effect [13]. In this case, the  $\theta$ -parameter is related to the Hall conductivity at the level of motion equations. Furthermore, applications of the Chern-Simons action have been discussed in several phenomena, such as superconductivity at high temperatures; fractional quantum Hall effect; anyons (particles with fractional statistics); and the Aharonov-Bohm effect.

Given the relevance of both PQED and the Chern-Simons action for planar systems, it is relevant to describe the competition between the  $\theta$ -parameter and the electromagnetic coupling constant, namely, the fine-structure constant  $\alpha$ . In this work, we show that the Chern-Simons parameter increases the dielectric constant, through the scale  $\alpha \rightarrow \alpha/(1 + \theta^2)$ , in the static limit. Within the dynamical regime, we apply the one-loop perturbation theory in our model, where we obtain: the electron mass renormalization; the quantum corrections for the electron  $g$ -factor; and the renormalization of the Fermi velocity.

The outline of this paper is the following: In Sec. II, we show the effective action for both, electromagnetic and statistical interactions. In Sec. III, we show the model, PQED with the Chern-Simons term. In Sec. IV, we calculate the static potential. In Sec. V, we calculate the electron self-energy for the isotropic case in one loop of perturbation theory. In Sec. VI, we calculate the renormalization of the Fermi velocity for high and low speeds using the renormalization group method. In Sec. VII, we review the main results obtained in this paper. We also include three Appendices. In App. A, we discuss the Maxwell-Chern-Simons theory. In App. B, we calculate the renormalized mass and in App. C we calculate the beta functions through the renormalization group for our model.

## II. EFFECTIVE ACTION FOR BOTH, ELECTROMAGNETIC AND STATISTICAL INTERACTIONS

In this section, we calculate both the electromagnetic and statistical interactions in the plane. In order to do so, let us consider the Euclidean version of the Chern-Simons theory in (2+1) dimensions, namely,

$$\mathcal{L}_{CS} = i\theta\epsilon_{\mu\nu\alpha}A_\mu\partial_\nu A_\alpha + ej_\mu A_\mu + \frac{\lambda}{2}\frac{A^\mu\partial_\mu\partial_\nu A^\nu}{(-\square)^{1/2}}, \quad (1)$$

where  $\theta$  is the Chern-Simons parameter,  $A_\mu$  is the statistical field,  $\square$  is the d'Alembertian operator, and  $j_\mu$  is the matter current [5]. The last term is included for calculating the gauge-field propagator. Eq. (1) yields an effective description for the Hall current at the level of motion equation [5].

Integration over  $A_\mu$  in Eq. (1) yields the effective action for the current matter  $j_\mu$ , i.e.,

$$\mathcal{L}_{\text{eff.}}^{\text{CS}}[j_\mu] = i\frac{e^2}{2\theta}j^\mu(x)\epsilon_{\mu\nu\alpha}\left[\frac{\partial^\alpha}{2(-\square)}\right]_{(x-y)}j^\nu(y), \quad (2)$$

which represents the statistical interaction [5] and we have taken into account the conservation of the current. Next, we review the effective electromagnetic interaction in the plane.

The PQED action reads

$$\mathcal{L}_{3D} = \frac{1}{2}F^{\mu\nu}(-\square)^{-1/2}F_{\mu\nu} + \frac{\lambda}{2}\frac{A^\mu\partial_\mu\partial_\nu A^\nu}{(-\square)^{1/2}} + ej^\mu A_\mu, \quad (3)$$

where  $F_{\mu\nu} = \partial_\mu A_\nu - \partial_\nu A_\mu$  with  $A_\mu$  being the pseudo electromagnetic field. Similarly to the previous calculation, we find

$$\mathcal{L}_{\text{eff.}}^{\text{PQED}}[j_\mu] = -\frac{e^2}{2}j^\mu(x)\left[\frac{1}{2(-\square)^{1/2}}\right]_{(x-y)}j_\mu(y). \quad (4)$$

Eq. (4) is the same effective action generated by quantum electrodynamics with particles confined to the plane [5]. In fact, this is the origin of the square root of  $\square$  in PQED. Here, our main goal is to obtain a model that describes at the same time both Eq. (2) and Eq. (4). Perhaps, the first attempt would be to consider the combination of quantum electrodynamics in (2+1) dimensions and the Chern-Simons theory coupled to the matter field. The resulting effective action, however, does not correctly describe either the electronic or the statistical interactions. We shall discuss this attempt in Appendix A.

## III. THE MODEL

We start with the action, in the Euclidean space, given by

$$\begin{aligned} \mathcal{L} = & \frac{1}{2}F^{\mu\nu}(-\square)^{-1/2}F_{\mu\nu} + \frac{\lambda}{2}A^\mu\partial_\mu(-\square)^{-1/2}\partial_\nu A^\nu \\ & + \mathcal{L}_M[\psi] + i\theta\epsilon_{\mu\nu\alpha}A^\mu\partial^\nu A^\alpha + ej^\mu A_\mu, \end{aligned} \quad (5)$$

where  $e$  is the electric charge,  $j_\mu = \bar{\psi}\gamma_\mu\psi$  is the matter current,  $\mathcal{L}_M[\psi]$  is the Dirac action for the matter field, explicitly  $\bar{\psi}(i\partial\!\!\!/ - m)\psi$ , and  $\lambda$  is a gauge-fixing parameter. The gamma matrix are rank 4 with  $(\gamma^0)^2 = (\gamma^1)^2 = (\gamma^2)^2 = -1$ , satisfying  $\{\gamma^\mu, \gamma^\nu\} = -2\delta^{\mu\nu}$ . Eq. (5) is meant to describe both the electromagnetic and statistical interactions, where the last is driven by the Chern-Simons term. We shall prove this claim by analyzing the effective action for the matter current.

Integrating out  $A_\mu$  in Eq. (5), we find the effective action for the matter current, namely,

$$\mathcal{L}_{\text{eff.}}[j_\mu] = -\frac{e^2}{2}j^\mu\Delta_{\mu\nu}^{(0)}j^\nu. \quad (6)$$

Note that the kind of  $\mathcal{L}_M[\psi]$  is needless for calculating Eq. (6).  $\Delta_{\mu\nu}^{(0)}$  is the gauge-field propagator, given by

$$\Delta_{\mu\nu}^{(0)} = \frac{\delta_{\mu\nu}}{2(-\square)^{1/2}(1+\theta^2)} - \frac{i\theta\epsilon_{\mu\nu\alpha}\partial^\alpha}{2(-\square)(1+\theta^2)} + \frac{1}{\lambda(-\square)^{1/2}} \frac{\partial_\mu\partial_\nu}{\square}. \quad (7)$$

Next, we use Eq. (7) in Eq. (6), yielding

$$\begin{aligned} \mathcal{L}_{\text{eff.}}[j_\mu] = & -\frac{e^2}{2(1+\theta^2)} j^\mu \left[ \frac{1}{2(-\square)^{1/2}} \right] j_\mu \\ & + \frac{ie^2\theta}{2(1+\theta^2)} j^\mu \epsilon_{\mu\nu\alpha} \partial^\alpha \left[ \frac{1}{2(-\square)} \right] j^\nu. \end{aligned} \quad (8)$$

Comparison with Eq. (2) and Eq. (4) shows that the first term on the right-hand side of Eq. (8) describes the electromagnetic interaction, while the second one yields the statistical interaction. Actually, for the sake of accuracy, we should consider a screening effect for the electric charge, namely,  $e^2/(1+\theta^2) \rightarrow e^2$  in order to obtain an exact correspondence. This shall be an important point for understading the role of  $\theta$  within our model. Eq. (8) has been obtained in Ref. [5], through a model that combines two gauge fields, where one yields the electromagnetic interaction and other is meant to describe the statistical field. In our model, the main difference is that we have obtained the same kind of effective action, but using only one gauge field, which shall be an useful description for including quantum corrections.

The Feynman rules for this model are the gauge-field propagator, in momentum space, given by

$$\Delta_{\mu\nu}^{(0)} = \frac{\delta_{\mu\nu}}{2(p^2)^{1/2}(1+\theta^2)} + \frac{\theta\epsilon_{\mu\nu\alpha}p^\alpha}{2p^2(1+\theta^2)} + \frac{1}{\lambda\sqrt{p^2}} \frac{p_\mu p_\nu}{p^2}. \quad (9)$$

In our calculations we shall use the Landau gauge ( $\lambda = \infty$ ). The electron-field propagator is

$$S_F^{(0)} = \frac{-1}{\gamma^\mu p_\mu - m} \quad (10)$$

and

$$\Gamma^\mu = e\gamma^\mu \quad (11)$$

is the vertex interaction. In the next section, we calculate the static potential for this model.

#### IV. STATIC INTERACTION

The Fourier transform of the static propagator of gauge field given by the Eq. (7), basically  $\Delta_{00}^{(0)}$ , generates the static potential  $V(r)$ , therefore,

$$V(r) = e^2 \int \frac{d^2k}{(2\pi)^2} \frac{\exp(-i\vec{k} \cdot \vec{r})}{2(|\vec{k}|^2)^{1/2}(1+\theta^2)}. \quad (12)$$

After solving the integration over the  $k$  [16], we have

$$V(r) = \frac{e^2}{4\pi(1+\theta^2)} \frac{1}{|\vec{r}|}. \quad (13)$$

For  $\theta = 0$ , we have the Coulomb potential, but for  $\theta \neq 0$ , we have an overall factor that behaves as an effective electric susceptibility. In Fig. 1, we plot this potential for

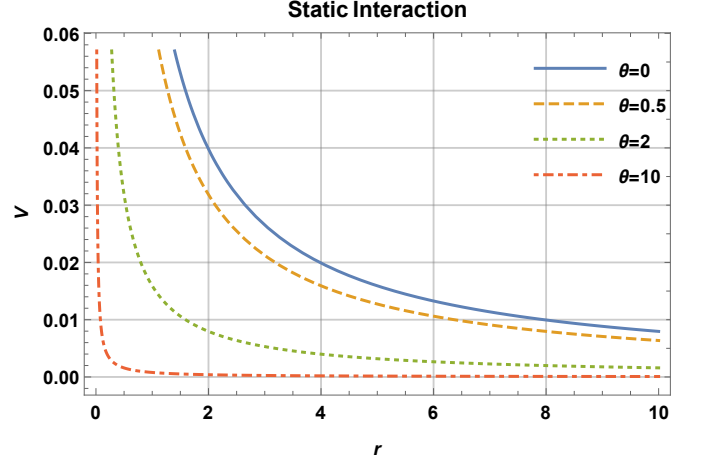


FIG. 1: Static potential of PQED coupled to the Chern-Simons action. This plot shows the behavior of the static potential Eq. (13) as a function of the distance between the fermions, varying the parameter  $\theta$ . The solid line (blue), dashed (orange), dotted (green) and dot-dashed (red) show the static potential as a function of the position for  $\theta = 0$ ,  $\theta = 0.5$ ,  $\theta = 2$  and  $\theta = 10$ , respectively.

some values of  $\theta$ . We conclude that for very large values of  $\theta$ , the electron-electron interaction becomes very weak in comparison with the unscreened Coulomb potential. This effect only occurs, within our model, because  $\theta$  is dimensionless.

#### V. THE ISOTROPIC SELF-ENERGIES

##### A. The fermion self-energy and the mass renormalization

The electron self-energy is given by

$$\Sigma(p, m) = e^2 \int \frac{d^Dk}{(2\pi)^D} \gamma^\mu S_F(p-k) \gamma^\nu \Delta_{\mu\nu}^{(0)}(k), \quad (14)$$

where  $D$  is the space-time dimension.

After using Eq. (9) in Eq. (14), we split the electron self-energy in two terms. In the first one contains the effects of PQED corrected by the factor  $1/(1+\theta^2)$  and the second one is the Chern - Simons contribution, namely,

$$\begin{aligned} \Sigma = & \frac{\Sigma_{\text{ISO}}^{\text{PQED}}}{(1+\theta^2)} + \\ & - \frac{\theta e^2 \epsilon_{\mu\alpha\nu}}{2(1+\theta^2)} \int \frac{d^Dk}{(2\pi)^D} \frac{(\gamma^\mu \not{p} \gamma^\nu - \gamma^\mu \not{k} \gamma^\nu + m \gamma^\mu \gamma^\nu)}{[(p-k)^2 + m^2]} \frac{k^\alpha}{k^2}, \end{aligned} \quad (15)$$

where  $\Sigma_{\text{ISO}}^{\text{PQED}}$  is the isotropic electron self-energy for

PQED is given by

$$\Sigma_{\text{ISO}}^{\text{PQED}} = e^2 \mu^\epsilon \int \frac{d^D k}{(2\pi)^D} \gamma^\mu S_F(p-k) \gamma^\nu \Delta_{\mu\nu}^{\text{PQED}}(k), \quad (16)$$

where  $\mu$  is the scale parameter,  $\epsilon$  is the dimensional regulator ( $\epsilon = 3 - D$ ),  $\Delta_{\mu\nu}^{\text{PQED}}$  is given by

$$\Delta_{\mu\nu}^{\text{PQED}} = \frac{\delta_{\mu\nu}}{2\sqrt{k^2}}, \quad (17)$$

and we use that  $e \rightarrow e\mu^{\epsilon/2}$ .

For calculating  $\Sigma_{\text{ISO}}^{\text{PQED}}$  we have used the Feynman's trick,

$$\frac{1}{ab^{1/2}} = \frac{1}{2} \int_0^1 dx \frac{(1-x)^{-1/2}}{[ax + b(1-x)]^{3/2}}, \quad (18)$$

where  $x$  is named Feynman's parameter and  $a$  and  $b$  are chosen as  $(p-k)^2 + m^2$  and  $b = k^2$ , respectively. Thereafter, using the dimensional regularization scheme [14], we find the isotropic electron self-energy for PQED,

$$\begin{aligned} \Sigma_{\text{ISO}}^{\text{PQED}} &= \frac{e^2}{8\pi^2} \int_0^1 dx (1-x)^{-1/2} (5(1-x)\not{p} - 3m) \frac{1}{\epsilon} + \\ &\quad - \frac{e^2}{16\pi^2} \int_0^1 dx (1-x)^{-1/2} \cdot \left[ \left( 2 + 5\gamma - 5 \ln \left( \frac{4\pi\mu^2}{\delta} \right) \right) (1-x)\not{p} + \right. \\ &\quad \left. + \left( 3 \ln \left( \frac{4\pi\mu^2}{\delta} \right) - 3\gamma - 2 \right) m \right], \end{aligned} \quad (19)$$

such that  $\delta = xm^2 + x(1-x)p^2$ ,  $\gamma$  is the Euler - Mascheroni constant ( $\sim 0.577$ ).

Next, we return to Eq. (15) for calculating the second term ( $\Sigma_{\text{CS}}$ ),

$$\Sigma_{\text{CS}} = -\frac{\theta e^2 \mu^\epsilon \epsilon_{\mu\alpha\nu}}{2(1+\theta^2)} \int \frac{d^D k}{(2\pi)^D} \frac{(\gamma^\mu \not{p} \gamma^\nu - \gamma^\mu \not{k} \gamma^\nu + m \gamma^\mu \gamma^\nu) k^\alpha}{[(p-k)^2 + m^2]} \frac{k^\alpha}{k^2}. \quad (20)$$

Using the following relation

$$\gamma^\mu \gamma^\nu \gamma^\alpha = \epsilon^{\mu\nu\alpha} - g^{\mu\nu} \gamma^\alpha - g^{\nu\alpha} \gamma^\mu + g^{\mu\alpha} \gamma^\nu, \quad (21)$$

we find

$$\Sigma_{\text{CS}} = \frac{\theta e^2 \mu^\epsilon}{2(1+\theta^2)} \int \frac{d^D k}{(2\pi)^D} \frac{(p \cdot k - k^2 + m \not{k})}{[(p-k)^2 + m^2] k^2}. \quad (22)$$

Next using another Feynman parametrization,

$$\frac{1}{ab} = \int_0^1 dy \frac{1}{[ax + b(1-x)]^2}, \quad (23)$$

we may rewrite  $\Sigma_{\text{CS}}$  as

$$\Sigma_{\text{CS}} = \frac{\theta e^2 \mu^\epsilon}{2(1+\theta^2)} \int_0^1 dx \int \frac{d^D k}{(2\pi)^D} \frac{x(1-x)p^2 + xm\not{p} - k^2}{[k^2 + \Delta]^2}, \quad (24)$$

where  $\Delta = xm^2 + x(1-x)p^2$ . We apply the dimensional regularization scheme for calculating the loop integral, hence,

$$\begin{aligned} \Sigma_{\text{CS}} &= \frac{\theta e^2}{16\pi(1+\theta^2)} \int_0^1 dx \frac{4x(1-x)p^2 + xm(\not{p} + 3m)}{[xm^2 + x(1-x)p^2]^{\frac{1}{2}}} \\ &= \frac{\theta e^2}{16\pi(1+\theta^2)} \{Am + B\not{p}\}, \end{aligned} \quad (25)$$

where

$$A = \frac{1}{m} \int_0^1 dx \frac{4x(1-x)p^2 + 3xm^2}{[xm^2 + x(1-x)p^2]^{\frac{1}{2}}} \quad (26)$$

and

$$B = \int_0^1 dx \frac{xm}{[xm^2 + x(1-x)p^2]^{\frac{1}{2}}}. \quad (27)$$

To obtain a finite amplitude, we use the minimal subtraction method, which consist of introducing counter-terms ( $CT$ ) in Eq. (15). Therefore, the renormalized electron self-energy reads

$$\Sigma^R = \lim_{\mu, \epsilon \rightarrow 0} (\Sigma(p, \mu, \epsilon) - CT) = C\not{p} + Dm, \quad (28)$$

where the coefficients  $C$  and  $D$  are expressed by

$$\begin{aligned} C &= -\frac{e^2}{16\pi^2(1+\theta^2)} \int_0^1 dx \left\{ \left[ 2 + 5\gamma + 5 \ln \left( \frac{\delta}{m^2} \right) \right] \sqrt{1-x} + \right. \\ &\quad \left. - \frac{xm\pi\theta}{[xm^2 + x(1-x)p^2]^{\frac{1}{2}}} \right\} \end{aligned} \quad (29)$$

and

$$\begin{aligned} D &= \frac{e^2}{16\pi^2(1+\theta^2)} \int_0^1 dx \left\{ \frac{[3\gamma + 2 + 3 \ln \left( \frac{\delta}{m^2} \right)]}{\sqrt{1-x}} + \right. \\ &\quad \left. + \frac{\pi\theta [4x(1-x)p^2 + 3xm^2]}{m[xm^2 + x(1-x)p^2]^{\frac{1}{2}}} \right\}. \end{aligned} \quad (30)$$

The renormalized mass  $m_R$  is given by the pole of the corrected propagator. Similarly to the calculation that has been done in [15], we found that the renormalized mass ratio is (for more details see Appendix B)

$$\begin{aligned} \frac{m_R}{m} &= 1 + C + D, \\ &= 1 - \frac{\alpha_{\text{eff}}^{\text{ISO}}}{4\pi} \int_0^1 dx \left\{ \frac{[\gamma + 2 \ln(x)](2-5x) - 2x}{\sqrt{1-x}} + \right. \\ &\quad \left. - \frac{4x^2\pi\theta}{\sqrt{2x-x^2}} \right\}, \end{aligned} \quad (31)$$

where  $m$  is the bare mass of the electron and  $\alpha_{\text{eff}}^{\text{ISO}} = e^2/4\pi(1+\theta^2)$ . Graphically, the renormalized mass ratio is shown in Fig. 2, where the global maximum value of renormalized mass was obtained at  $\theta \cong 0.36$ . Furthermore, for large values of  $\theta$  the mass does not renormalize.

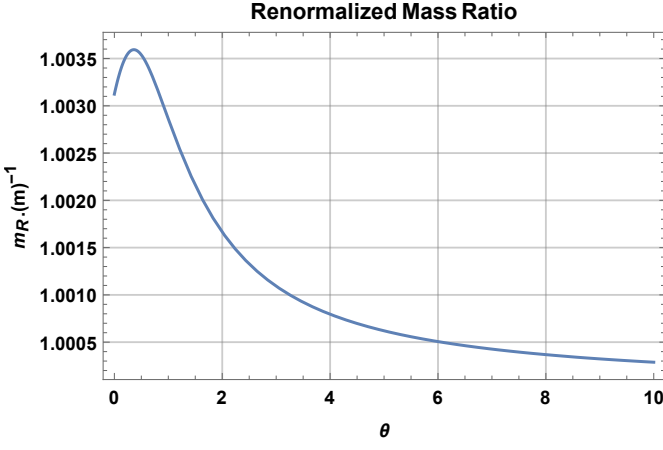


FIG. 2: The variation of renormalized mass ratio with  $\theta$ . This plot shows the behavior of the variation of renormalized mass ratio Eq. (31) as a function of  $\theta$ , considering  $e^2/4\pi = 1/137$ .

### B. The photon self-energy and screened static interaction

The full propagator of the gauge field, considering the insertion of the photon self-energy [7], is given by

$$\Delta_{\mu\nu}^{\text{Full}}(p) = \frac{\sqrt{p^2} \left[ 2(1 + \theta^2) + \frac{e^2}{8} \right] P_{\mu\nu} + 2\theta(1 + \theta^2)\epsilon_{\mu\nu\lambda}p^\lambda}{p^2 \left[ 2(1 + \theta^2) + \frac{e^2}{8} \right]^2}, \quad (32)$$

where  $P_{\mu\nu}$  is called the transverse operator, given by  $P_{\mu\nu} = \delta_{\mu\nu} - p_\mu p_\nu / p^2$ . Note that we have used the four-rank representation of the Dirac matrices in Eq. (32).

In the static limit, within the Landau gauge, the gauge-field propagator reads

$$\Delta_{00}^{\text{Full}}(\mathbf{p}) = \frac{1}{2\sqrt{\mathbf{p}} \left( 1 + \theta^2 + \frac{e^2}{16} \right)}. \quad (33)$$

After solving the Fourier transform of the static propagator, we find the potential

$$V(r) = \frac{e^2}{4\pi \left( 1 + \theta^2 + \frac{e^2}{16} \right)} \frac{1}{|\vec{r}|}. \quad (34)$$

Eq. (34) yields the total screening effect of the potential. Therefore, we have shown that the whole description of the screening depends on both the statistical parameter  $\theta$  and the quantum corrections given by the factor  $e^2/16$ . This indicates that large values of the effective dielectric constant may be obtained in experiments.

In the next section, we calculate the anisotropic self-energy and the Fermi velocity renormalization for high and low-speed regimes.

## VI. THE ANISOTROPIC SELF-ENERGY AND THE FERMI VELOCITY RENORMALIZATION

Let us consider a soft breaking of the Lorentz symmetry [17] in the fermionic sector given by the following Lagrangean

$$\mathcal{L} = \frac{1}{2} F^{\mu\nu} (-\square)^{-1/2} F_{\mu\nu} + \frac{\lambda}{2} A^\mu \partial_\mu (-\square)^{-1/2} \partial_\nu A^\nu + \bar{\psi} (i\gamma^0 \partial_0 + i v_F \gamma^i \partial_i - m) \psi + i\theta \epsilon_{\mu\nu\alpha} A^\mu \partial^\nu A^\alpha + e j^\mu A_\mu. \quad (35)$$

Note that, in this case the fermion propagator Eq. (10) is

$$S_F^{(0)}(p) = \frac{\gamma^\mu \bar{p}_\mu + m}{\bar{p}^2 + m^2}, \quad (36)$$

where  $\bar{p}^\mu = (p_0, v_F \mathbf{p})$  and  $\bar{p}^2 = p_0^2 + v_F^2 \mathbf{p}^2$ . The photon propagator reads

$$\Delta_{\mu\nu}^{(0)}(p) = \frac{\delta_{\mu\nu}}{2(p^2)^{1/2}(1 + \theta^2)} + \frac{i\theta \epsilon_{\mu\nu\alpha} p^\alpha}{2p^2(1 + \theta^2)}, \quad (37)$$

where we adopted the Landau gauge ( $\lambda = \infty$ ),  $p^\mu = (p_0, \mathbf{p})$  and  $p^2 = p_0^2 + \mathbf{p}^2$ , as well as the vertex structure Eq. (38) becomes

$$\Gamma^\mu = e (\gamma^0, v_F \gamma^i). \quad (38)$$

Note that in this section we consider  $c = 1$ , for simplicity.

The electron self-energy is given by

$$\Sigma(p) = e^2 \int \frac{d^D k}{(2\pi)^D} \Gamma^\mu S_F(\bar{p} - \bar{k}) \Gamma^\nu \Delta_{\mu\nu}(k). \quad (39)$$

From Eq. (39), it is possible to split the electron self-energy in two terms. The first one contains the effects of PQED with the overall factor  $1/(1 + \theta^2)$  and the second one is the additional Chern-Simons contribution, hence,

$$\Sigma(p) = \frac{\Sigma_{\text{ANI}}^{\text{PQED}}}{(1 + \theta^2)} + \frac{\theta e^2}{(1 + \theta^2)} \epsilon_{\mu\alpha\nu} \int \frac{d^D k}{(2\pi)^D} \frac{(\gamma^\mu \bar{p} \gamma^\nu - \gamma^\mu \bar{k} \gamma^\nu - m \gamma^\mu \gamma^\nu) k^\alpha}{[(\bar{p} - \bar{k})^2 + m^2]} \frac{k^\alpha}{k^2}. \quad (40)$$

In what follows, we will calculate these diagrams using the dimensional regularisation procedure as a way to obtain finite Feynman amplitudes. We first perform the integration over  $k_0$  and then the one over  $\mathbf{k}$  using standard formulas of dimensional regularization in spatial dimension  $d = 2 - \epsilon$ . We also use that  $e \rightarrow e^{\mu/2}$

Note that the integrals in the second term Eq. (40) are finite. Hence, using the method of renormalization group (see Appendix C), we conclude that this term does not

contribute to the Fermi velocity renormalization.  $\Sigma_{\text{ANI}}^{\text{PQED}}$  is the anisotropic electron self-energy for PQED, given by

$$\begin{aligned}\Sigma_{\text{ANI}}^{\text{PQED}}(p) &= e^2 \int \frac{d^D k}{(2\pi)^D} \gamma^\mu S_F(\bar{p} - \bar{k}) \gamma^\nu \Delta_{\mu\nu}(k) \\ &= \frac{e^2}{8\pi^2} \left\{ (1 - 2v_F^2) \gamma^0 p_0 I_1 + \right. \\ &\quad \left. + (1 + 2v_F^2) m I_2 + v_F \gamma^i p_i I_3 \right\} \frac{1}{\epsilon},\end{aligned}\quad (41)$$

where

$$\begin{aligned}I_1 &= \int_0^1 dx \frac{(1-x)^{1/2}}{x(1-v_F^2)-1}, \\ I_2 &= \int_0^1 dx \frac{(1-x)^{-1/2}}{x(1-v_F^2)-1}, \\ I_3 &= \int_0^1 dx \frac{(1-x)^{-1/2} \left(1 + \frac{x\beta^2}{x(1-v_F^2)-1}\right)}{x(1-v_F^2)-1}.\end{aligned}\quad (42)$$

Therefore, the running Fermi velocity  $\beta_{v_F}$  may be written as

$$\begin{aligned}\beta_{v_F} &= \frac{e^2}{8\pi^2(1+\theta^2)} [I_3 + (1 - 2v_F^2)I_1] \\ &= -\frac{e^2}{8\pi^2(1+\theta^2)} \times \\ &\quad \int_0^1 dx \frac{\sqrt{1-x}}{1-x(1-v_F^2)} \left[ 1 - 2v_F^2 + \frac{1}{1-x(1-v_F^2)} \right],\end{aligned}\quad (43)$$

where  $\beta_{v_F} = \mu(\partial v_F^R / \partial \mu)$  and  $\mu$  is the energy scale parameter.

In the low-velocity regime  $v_F \ll 1$ , the lowest order term in Eq. (43) reads

$$\beta_{v_F} = -\frac{e^2}{16\pi(1+\theta^2)}.\quad (44)$$

By solving Eq. (44), we find the renormalized Fermi velocity, namely,

$$v_F^R(\mu) = v_F \left[ 1 - \frac{\alpha_{\text{eff}}}{4} \ln \left( \frac{\mu}{\mu_0} \right) \right],\quad (45)$$

where

$$\alpha_{\text{eff}} = \frac{e^2}{4\pi v_F(1+\theta^2)}.\quad (46)$$

From Eq. (45) is clear that for this theory, the Fermi velocity renormalization is controlled by Chern-Simons parameter. For  $\theta$  equal zero, the  $v_F^R$  is the well-known result, caculated in Ref. [18]. Nevertheless, for large values of  $\theta$ , the Fermi velocity does not renormalize, remaning close to its bare value, see Fig. 3

In the high-velocity regime  $v_F \sim 1$ , until the first order in  $(1 - v_F)$ ,  $\beta_{v_F}$  becomes

$$\beta_{v_F} = -\frac{2e^2}{5\pi^2(1+\theta^2)}(1 - v_F).\quad (47)$$

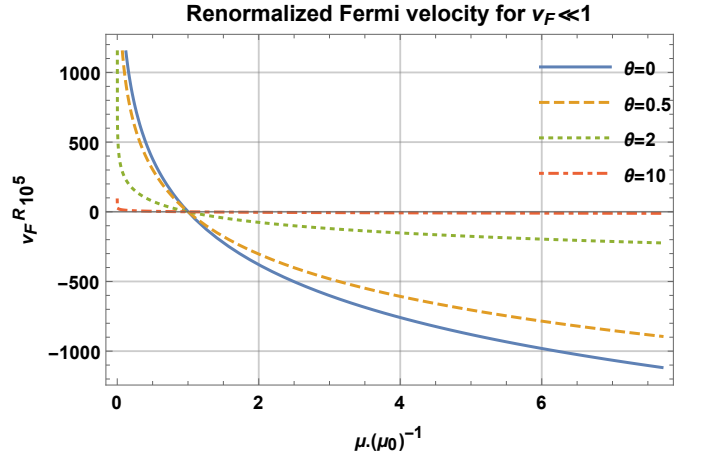


FIG. 3: The renormalized Fermi velocity for  $v_F \ll 1$ . This plot shows the behavior of the renormalized Fermi velocity Eq. (45) as a function of  $\mu/\mu_0$ , varying the parameter  $\theta$ , where the solid line (blue), dashed (orange), dotted (green) and dot-dashed (red) are for  $\theta = 0$ ,  $\theta = 0.5$ ,  $\theta = 2$  and  $\theta = 10$ , respectively.

Hence, the Fermi velocity for  $v_F \sim 1$  is

$$v_F^R(\mu) = \left[ 1 - (1 - v_F) \left( \frac{n}{n_0} \right)^{\frac{\gamma}{2}} \right],\quad (48)$$

where  $\gamma = \frac{8v_F\alpha_{\text{eff}}}{5\pi}$  and we have used the relation  $\mu/\mu_0 \rightarrow (n/n_0)^{1/2}$  [19], with  $n$  and  $n_0$  being the density of states.

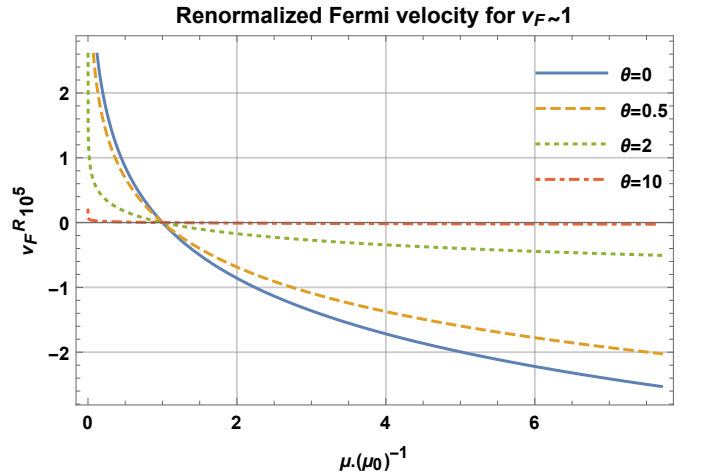


FIG. 4: The renormalized Fermi velocity for  $v_F \sim 1$ . This plot shows the behavior of the renormalized Fermi velocity Eq. (48) as a function of  $\mu/\mu_0$ , varying the parameter  $\theta$ , where the solid line (blue), dashed (orange), dotted (green) and dot-dashed (red) are for  $\theta = 0$ ,  $\theta = 0.5$ ,  $\theta = 2$  and  $\theta = 10$ , respectively.

In the limit of large values of  $\theta$  the Fermi velocity does not renormalize, see Fig. 4. Note also that for  $n = 0$  [20], the low-density regime, the Fermi velocity renormalize to  $c = 1$ . This result implies that the renormalized Fermi

velocity does not diverge at zero doping, instead of the corresponding result in Eq. (45).

## VII. DISCUSSION

Planar-field theories are the ideal platform for investigating electronic interactions in two-dimensional materials at low energies. The well-developed methods of quantum field theory for calculating quantum corrections, dynamical symmetry breaking, and anomalies make this idea more exciting yet. However, the full description of these systems is a hard task, mainly because of several kinds of interactions that emerge due to the lattice vibrations, disorder, and impurities just to cite a few. Aiming to this direction, PQED has been investigated together with a Gross-Neveu interaction, which is expected to describe either phonons or impurities at low energies [7]. Beyond all of these microscopic interactions, we also have the challenge of describing the topological effects driven by the Chern-Simons action.

In the present work we have shown that, because the Chern-Simons parameter is dimensionless, most of its effects may be absorbed by a simple scaling of the fine-structure constant in the static limit. Therefore, we find a model that provides any dielectric constant depending on the value of  $\theta$ . This may be realized experimentally by placing the material above some substrate. Furthermore, in the dynamical limit, the  $\theta$ -parameter changes the electron bare mass, yielding a maximal value at  $\theta \approx 1$ . Thereafter, we have calculated the renormalized Fermi velocity in both static and dynamical regimes. In these cases, the main role of  $\theta$  is to yield a screened dielectric constant. Finally, we have shown that  $\theta$  changes the value of the corrected electron  $g$ -factor. Indeed, it has been shown that for  $\theta = 0$  this quantity has a good agreement with the experimental data [9]. For consistency, our result also yields a good comparison because the  $\theta$ -parameter works as a fixing parameter for taking into account the effects of the substrate, which has to be considered for comparison with experimental data. All of these results are dependent on the one-loop perturbation theory, but our model is likely to provide new physics in other regimes, for instance, in the strong-coupling limit or when fermions are coupled to an external magnetic field. These limits are relevant to investigating a dynamical symmetry breaking and fractional quantum Hall effect, respectively. We shall investigate these cases elsewhere.

After coupling PQED to the Chern-Simons action, we prove that both statistical and electromagnetic actions surprisingly remain unchanged. This is an exact result because the model is quadratic in the gauge field  $A_\mu$ . It is important to address that this has been made with the only *one* gauge field, instead of adding a new statistical field, as it has been done in Ref. [5]. In other words, we have a model that *simultaneously* describes both electron-electron interactions and the statistical interac-

tion between the matter current. This may be appropriate for calculating properties of the fractional quantum Hall effect, considering that the Coulomb potential plays some role in describing this effect. In Ref. [21], the author has investigated this possibility by using a multicomponent Chern-Simons theory, which interacts with electrons in the presence of an external magnetic applied to a graphene sheet. Furthermore, these electrons also interact through the repulsive Coulomb potential. A possible generalization of this model into the dynamical limit is straightforwardly obtained from our approach. Dynamical effects of PQED, related to topological phases and dynamical mass generation, have been calculated in Ref. [8].

## Acknowledgments

G. C. M. is partially supported by Coordenação de Aperfeiçoamento de Pessoal de Nível Superior – Brasil (CAPES), finance code 001; V. S. A. is partially supported by Conselho Nacional de Desenvolvimento Científico e Tecnológico (CNPq) and by CAPES/NUFFIC, finance code 0112; E. C. M. is partially supported by both CNPq and Fundação Carlos Chagas Filho de Amparo à Pesquisa do Estado do Rio de Janeiro (FAPERJ); L. O. N. is partially supported by CAPES/NUFFIC, finance code 0112.

## Appendix A: Maxwell-Chern-Simons Action

In this appendix we calculate the effective action for the matter current coupled to the Maxwell-Chern-Simons gauge field. Thereafter, we investigate the static limit of this model. We start with the action, given by

$$\mathcal{L}_{\text{QED}} = \frac{1}{4} F^{\mu\nu} F_{\mu\nu} + \lambda A^\mu \partial_\mu \partial_\nu A^\nu + \mathcal{L}_M[\psi] + i\theta \epsilon_{\mu\nu\alpha} A^\mu \partial^\nu A^\alpha + e j^\mu A_\mu, \quad (49)$$

where  $A_\mu$  is the Maxwell field. Integration over  $A_\mu$  yields

$$\mathcal{L}_{\text{eff.}}^{\text{QED}}[j_\mu] = -\frac{e^2}{2} j^\mu \left[ \frac{1}{-\square + 4\theta^2} \right] j_\mu + i \frac{e^2 \theta}{2} j^\mu \epsilon_{\mu\nu\alpha} \partial^\alpha \left[ \frac{1}{\square(-\square + 4\theta^2)} \right] j^\nu. \quad (50)$$

It's not surprising that the first term in the rhs of Eq. (50) does not provide the proper electromagnetic effective action, which is given by PQED. The effect on the statistical interaction, nevertheless, is more dramatic. Indeed, this interaction is proportional to  $\square^{-1}$  in Eq. (2). Here, it is modified to  $\square^{-1}(-\square + 4\theta^2)^{-1}$ , which yields some different kind of interaction. This occurs because  $\theta$  has the dimension of mass in Eq. (49). For PQED, nevertheless,  $\theta$  is dimensionless. We may estimate the

effect of a massive  $\theta$  by calculating the static limit. In this case, the static potential generated by the model in Eq. (49) is

$$V(r) = \frac{e^2}{2\pi} K_0(r\theta), \quad (51)$$

where  $K_0(r\theta)$  is the modified Bessel function of the second kind. For  $r\theta \ll 1$ , we have  $V(r) \propto \ln(r\theta)$ , while for  $r\theta \gg 1$ , we find  $V(r) \propto e^{-r\theta}/\sqrt{r\theta}$ . It is clear that  $1/\theta$  plays the role of an interaction length, wherein the short-range limit we have a logarithmic-confining potential. On the other hand, in the long-range limit, we find an exponential potential which quickly goes to zero. This resembles the Meissner effect in superconductors.

The main goal of this appendix is to clarify the relevance of our model in Eq. (5). Indeed, it is remarkable that PQED coupled to the Chern-Simons action provides a simultaneous description for both electromagnetic and statistical interactions in the light of the effective action for the matter current.

### Appendix B: Mass renormalization

In this appendix we derive Eq. (31) that yields the physical mass. This renormalized mass  $m_R$  is given by the pole of the corrected propagator, given by

$$S_F^R = \frac{-1}{\not{p} - m - \Sigma^R(\not{p}, m)}. \quad (52)$$

Using Eq. (28) in Eq. (52), we find

$$S_F^R = \frac{-1}{(1-C)\not{p} - (1+D)m}, \quad (53)$$

where  $C$  and  $D$  are functions of  $p$  and  $m$  given by Eq. (29) and Eq. (30), respectively. Furthermore, they are proportional to  $e^2$  within our one-loop approximation. From Eq. (53), we conclude that the pole of the propagator reads  $p^2 = m^2(1+D)^2/(1-C)^2$ . Within the one-loop approximation, this can be rewritten as  $p^2 = M^2(p, m)$ , where  $M(p, m) = 1 + C + D$  is called mass function. Therefore, the renormalized mass, in the mass shell, is given by

$$m_R = M(p^2 = -m^2) = 1 + C + D, \quad (54)$$

which is our desired result in Eq. (31). Note that to find the renormalized mass it is necessary to return to Minkowski space, for more details regarding this approximation see [15].

### Appendix C: Renormalization Group Functions

The vertex functions, which have been made finite by the subtraction of the pole terms in the dimensionally regularized amplitudes, satisfy a 't Hooft-Weinberg

renormalization group equation:

$$\left( \mu \frac{\partial}{\partial \mu} + \beta_e \frac{\partial}{\partial e} + \beta_{v_F} \frac{\partial}{\partial v_F} - N_F \gamma_\psi - N_A \gamma_A \right) \Gamma^{(N_F, N_A)} = 0, \quad (55)$$

where we have considered the massless case. Here,  $\Gamma^{(N_F, N_A)} = \Gamma^{(N_F, N_A)}(p_i, \mu, e, v_F)$  denotes the renormalized vertex function of  $N_F$  fermion fields and  $N_A$  gauge fields, and  $p_i$  denotes the external momenta. We have introduced the renormalization scale  $\mu$  through the substitution  $e \rightarrow \mu^{\epsilon/2} e$ , where  $\epsilon = 2 - d$ . The  $\beta_i$ 's for  $i = e, v_F$  are the beta functions which describe how the electric charge, Fermi velocity change with the scale parameter  $\mu$  and are usually defined as  $\beta_e = \mu \frac{\partial e}{\partial \mu}$ ,  $\beta_{v_F} = \mu \frac{\partial v_F}{\partial \mu}$ .

The functions  $\gamma_\psi$  and  $\gamma_A$  are the anomalous dimensions of the fields  $\psi$  and  $A_\mu$  and given by  $\gamma_\psi = \mu \frac{\partial}{\partial \mu} (\ln \sqrt{Z_\psi})$  and  $\gamma_A = \mu \frac{\partial}{\partial \mu} (\ln \sqrt{Z_A})$ , where  $Z_\psi$  and  $Z_A$  are the wave function renormalization of the fields  $\psi$  and  $A_\mu$ , respectively.

To remove the pole term in the amplitudes  $I^{(N_F, N_A)}$  contained in  $\Gamma^{(N_F, N_A)}$ , we use the following prescription

$$(1 - \mathcal{T}) \mu^{x\epsilon} I^{(N_F, N_A)} = \text{Finite}^{(N_F, N_A)} + x \ln \mu \text{Res}^{(N_F, N_A)},$$

where  $\mathcal{T}$  is an operator used to remove the pole term. In the above expression,  $\text{Res}^{(N_F, N_A)}$  means residue of the diagram that is given by the coefficient of the term  $1/\epsilon$ , and  $\text{Finite}^{(N_F, N_A)}$  is the finite part of the amplitudes  $I^{(N_F, N_A)}$ .

By performing the calculations up to one loop, we find

$$\Gamma^{(2,0)}(\bar{p}) = \gamma^\mu \bar{p}_\mu + \Sigma(\bar{p}), \quad (56)$$

where  $\Sigma(\bar{p}) = \frac{e^2}{1+\theta^2} [\text{Finite}^{(2,0)} + \ln \mu \text{Res}^{(2,0)}]$ , and  $\text{Res}^{(2,0)} = A_1 \gamma^0 p_0 + A_2 \gamma^i p_i$ .

After writing the RG functions perturbatively as,  $\beta_i = \sum_{j=1}^2 \beta_i^{(j)} e^j$ , we find that in order of  $e$ ,

$$\gamma_\psi^{(1)} = 0, \quad \beta_{v_F}^{(1)} = 0, \quad \beta_e^{(1)} = 0, \quad .$$

On the other hand, in order  $e^2$  we find

$$\gamma_\psi^{(2)} = \frac{1}{2} A_1, \quad \beta_{v_F}^{(2)} = A_2 + v_F A_1, \\ \beta_e^{(2)} = \gamma_A^{(1)}, \quad .$$

However, because the polarization tensor is finite in one-loop (order  $e^2$ ) and accordingly  $\beta_e = 0$ .

Finally, we may identify through the Feynman diagrams that

$$A_1 = \frac{1}{8\epsilon\pi^2(1+\theta^2)} (1 - 2v_F^2) I_1, \\ A_2 = \frac{1}{8\epsilon\pi^2(1+\theta^2)} v_F I_3,$$

and we obtain

$$\beta_{v_F} = \frac{e^2}{8\epsilon\pi^2(1+\theta^2)} [(1 - 2v_F^2) I_1 + v_F I_3], \quad (57)$$



From equation  $\beta_{v_F} = \mu \frac{\partial v_F^R}{\partial \mu}$ , the flow of the effective Fermi velocity can be written as:

$$\frac{\partial v_F^R(\mu)}{\partial t} = \beta_{v_F}(\beta), \quad (58)$$

where  $v_F(t=0) = v_F(\mu_0)$ , and we have introduced a

logarithmic scale  $t = \ln(\mu/\mu_0)$ , with  $\mu_0$  a reference scale where the parameter  $v_F^0$  has been defined.

Using Eq. (43) in  $v_F \ll 1$  regime in Eq. (57) we find Eq. (45). In the same way taking Eq.(67) from Eq. (43) we find Eq. (48).

- 
- [1] K. S. Novoselov, A. K. Geim, S. V. Morozov, D. Jiang, Y. Zhang, S. V. Dubong, I. V. Grigorieva, and A. A. Firsov, *Electric Field Effect in Atomically Thin Carbon Films*, Science **306**, 666, (2004).
- [2] A. H. Castro Neto, F. Guinea, N. M. R. Peres, K. S. Novoselov, and A. K. Geim, *The Electronic Properties of Graphene*, Rev. Mod. Phys. **81**, 109 (2009).
- [3] M. I. Katsnelson, K. S. Novoselov, and A. K. Geim, *Chiral tunnelling and the Klein Paradox in Graphene*, Nat. Phys. **2**, 620 (2006).
- [4] B. Lalmi, H. Oughaddou, H. Enriquez, A. Kara, S. Vizzini, B. Ealet, and B. Aufray, *Epitaxial growth of a silicene sheet*, Appl. Phys. Lett. **97**, 223109 (2010); L. Li, Y. Yu, G. J. Ye, Q. Ge, X. Ou, H. Wu, D. Feng, X. H. Chen, and Y. Zhang, *Black Phosphorus field-effect Transistors*, Nat. Nanotech. **9**, 372, (2014); X.-S. Ye, Z.-G. Shao, H. Zhao, L. Yang, and C.-L. Wang, *Intrinsic carrier mobility of germanene is larger than graphene's: first-principle calculations*, RSC Adv. **4**, 21216-21220, (2014); Q. H. Wang, K. K.-Zadeh, A. Kis, J. N. Coleman, and M. S. Stran, *Electronics and Optoelectronics of Two-dimensional Transition Metal Dichalcogenides*, Nat. Nanotech. **7**, 699, (2012).
- [5] E. C. Marino, *Quantum Electrodynamics of Particles on a Plane and the Chern-Simons Theory*, Nucl. Phys. B **408**, 551-564 (1993).
- [6] E. C. Marino, Leandro O. Nascimento, Van Sérgio Alves, and C. Morais Smith, *Unitarity of Theories Containing Fractional Powers of the d'Alembertian Operator*, Phys. Rev. D **90**, 105003 (2014).
- [7] V. S. Alves, W. S. Elias, L. O. Nascimento, V. Juričić and F. Peña, *Chiral Symmetry Breaking in the Pseudo-Quantum Electrodynamics*, Phys. Rev. D **87**, 125002 (2013); L. O. Nascimento, V. S. Alves, F. Peña, C. M. Smith, and E. C. Marino, *Chiral-symmetry breaking in pseudoquantum electrodynamics at finite temperature*, Phys. Rev. D, **92**, 025018 (2015); V. S. Alves, R. O. C. Junior, E. C. Marino, and L. O. Nascimento, *Dynamical Mass Generation in Pseudo Quantum Electrodynamics with Four-Fermion Interactions*, Phys. Rev. D **96**, 034005 (2017).
- [8] E. C. Marino, L. O. Nascimento, V. S. Alves, and C. M. Smith, *Interaction Induced Quantum Valley Hall Effect in Graphene*, Phys. Rev. X **5**, 011040 (2015).
- [9] N. Menezes, V. S. Alves, E. C. Marino, L. Nascimento, L. O. Nascimento, and C. M. Smith, *Spin g-factor due to electronic interactions in graphene*, Phys. Rev. B **95**, 245138 (2017).
- [10] V. S. Alves, T. Macrì, G. C. Magalhães, E. C. Marino, and L. O. Nascimento, *Two-dimensional Yukawa interactions from nonlocal Proca quantum electrodynamics*, Phys. Rev. D **97**, 096003 (2018).
- [11] E. C. Marino, Leandro O. Nascimento, Van Sérgio Alves, N. Menezes, C. Morais Smith, *Quantum-electrodynamical approach to the exciton spectrum in Transition-Metal Dichalcogenides*, 2D Mater. **5**, 041006 (2018).
- [12] G. V. Dunne, *Aspects of Chern-Simons Theory*, Springer-Verlag, 179 (1999).
- [13] B. A. Bernevig with T. Hughes, *Topological Insulators and Topological Superconductors*. Princeton University Press, (2013); S.-Q. Shen, *Topological Insulators Dirac Equation in Condensed Matter*, Spring Series in Solid-State Sciences, (2012); M. Z. Hasan and C. L. Kane, *Colloquium: Topological Insulators*, Rev. Mod. Phys. **82**, 3045, (2010).
- [14] C. G. Bollini, J. J. Giambiagi, *Lowest order "divergent" graphs in  $\nu$ -dimensional space*, Phys. Lett. B **40**, 566 (1972); G. t'Hooft, M. Veltman, *Regularization and Renormalization of Gauge Fields*, Nucl. Phys.B **44**, 189 (1972); J. F. Ashmore, *A method of gauge-invariant regularization*, Lett. Nuovo Cimento **4**, 289 (1972).
- [15] V. S. Alves, T. Macrì, G. C. Magalhães, L. O. Nascimento, *Two-dimensional Yukawa interactions from non-local Proca quantum electrodynamics*, Phys. Rev. D **97**, 096003 (2018);
- [16] I. S. Gradshteyn and I. M. Ryzhik, *Table of Integrals, Series and Products*, 7th ed. (Academic Press, New York, 2007).
- [17] P. R. S. Gomes, M. Gomes *Higher spatial derivative field theories*, Phys. Rev. D **85**, 085018 (2012).
- [18] M. A. H. Vozmediano *Renormalization group aspects of graphene*, Phil. Trans. R. Soc. A (2011) 369.
- [19] D. C. Elias, R. V. Gorbachev, A. S. Mayorov, et al., *Dirac cones reshaped by interaction effects in suspended graphene*, Nature Physics **7**, 701 (2011).
- [20] E. C. Marino, *Quantum Field Theory Approach to Condensed Matter Physics*, Cambridge University Press, 2017
- [21] C. Fräßdorf, *Abelian Chern-Simons theory for the fractional quantum Hall effect in graphene*, Phys. Rev. B **97**, 115123 (2018).